

Fluorocoxib A enables targeted detection of cyclooxygenase-2 in laser-induced choroidal neovascularization

Md. Jashim Uddin
Chauca E. Moore
Brenda C. Crews
Cristina K. Daniel
Kebreab Ghebreselasie
J. Oliver McIntyre
Lawrence J. Marnett
Ashwath Jayagopal

Fluorocoxib A enables targeted detection of cyclooxygenase-2 in laser-induced choroidal neovascularization

Md. Jashim Uddin,^{a,*} Chauca E. Moore,^b
Brenda C. Crews,^a Cristina K. Daniel,^a
Kebreab Ghebreselasie,^a J. Oliver McIntyre,^c
Lawrence J. Marnett,^a and Ashwath Jayagopal^{b,d}

^aVanderbilt University School of Medicine, Vanderbilt-Ingram Cancer Center, Vanderbilt Institute of Chemical Biology, Department of Biochemistry, Chemistry and Pharmacology, A. B. Hancock, Jr., Memorial Laboratory for Cancer Research, Nashville, Tennessee 37232-0146, United States

^bVanderbilt University School of Medicine, Vanderbilt Eye Institute, Department of Ophthalmology and Visual Sciences, Nashville, Tennessee 37232-6840, United States

^cVanderbilt University School of Medicine, Vanderbilt-Ingram Cancer Center, Department of Cancer Biology, Nashville, Tennessee 37232-6840, United States

^dPharma Research and Early Development, Roche Innovation Center Basel, F. Hoffmann-La Roche Ltd., Basel 4070, Switzerland

Abstract. Ocular angiogenesis is a blinding complication of age-related macular degeneration and other retinal vascular diseases. Clinical imaging approaches to detect inflammation prior to the onset of neovascularization in these diseases may enable early detection and timely therapeutic intervention. We demonstrate the feasibility of a previously developed cyclooxygenase-2 (COX-2) targeted molecular imaging probe, fluorocoxib A, for imaging retinal inflammation in a mouse model of laser-induced choroidal neovascularization. This imaging probe exhibited focal accumulation within laser-induced neovascular lesions, with minimal detection in proximal healthy tissue. The selectivity of the probe for COX-2 was validated *in vitro* and by *in vivo* retinal imaging with nontargeted 5-carboxy-X-rhodamine dye, and by blockade of the COX-2 active site with nonfluorescent celecoxib prior to injection of fluorocoxib A. Fluorocoxib A can be utilized for imaging COX-2 expression *in vivo* for further validation as an imaging biomarker in retinal diseases. © 2016 Society of Photo-Optical Instrumentation Engineers (SPIE) [DOI: 10.1117/1.JBO.21.9.090503]

Keywords: cyclooxygenase-2; fluorocoxib A; laser-induced choroidal neovascularization; optical imaging.

Paper 160251LR received Apr. 19, 2016; accepted for publication Aug. 26, 2016; published online Sep. 14, 2016.

Ocular neovascularization is a key blinding complication of neovascular age-related macular degeneration (AMD), a major cause of irreversible vision loss in the elderly population.^{1,2}

In neovascular AMD, the abnormal growth of subretinal neovessels damages the retinal architecture, resulting in death of cells, and loss of central vision. Strategies for early detection of vascular disease, particularly ocular inflammatory processes that are thought to precede angiogenesis,³ are needed in the clinic to enable timely therapeutic intervention prior to the onset of vision-threatening disease progression. Inflammation has been reported to be a major driver of AMD disease progression, and anti-inflammatory therapies are under investigation to treat intermediate forms of AMD, with the intent of halting disease progression to the neovascular stage.⁴ Therefore, molecular imaging strategies capable of detecting inflammatory mediators such as cytokines, leukocyte biomarkers, and enzymes are of particular value in ophthalmology.

Previous studies have associated the expression of the inflammatory enzyme cyclooxygenase-2 (COX-2) with increased susceptibility for the development of choroidal neovascularization in neovascular AMD using human ocular specimens.⁵ In addition, we have previously demonstrated the utility of a fluorescent conjugate of indomethacin, fluorocoxib A, for imaging COX-2 using *in vivo* tumor models with high selectivity.⁶ Therefore, in this study, we investigated the feasibility of using fluorocoxib A for detection of COX-2 in retinal vascular tissues, using an established mouse model of neovascular AMD. Specifically, the mouse model of laser-induced choroidal neovascularization (LCNV) was used to model early inflammation with subsequent angiogenesis, and thus exhibits several major pathologic components of human neovascular AMD. Fluorocoxib A fluorescence was visualized in LCNV models during early inflammatory stages of pathology that precede angiogenesis, thus allowing us to conduct a proof of concept study demonstrating COX-2 expression prior to neovascularization in this model.

As demonstrated by spectrofluorometry, both fluorocoxib A and the nontargeted 5-carboxy-X-rhodamine dye (5-ROX) exhibited red-shifted fluorescence excitation (λ_{ex}) and emission (λ_{em}) (Fig. 1). To measure the quantum yield (ϕ) of fluorocoxib A, fluorescence excitation and emission spectra of both fluorocoxib A and 5-ROX, each diluted to $\sim 1 \mu\text{M}$ (optical density $\sim 0.04/\text{cm}$, $10 \times 4 \text{ mm}$ cuvettes), were recorded in triplicate and at ambient temperature ($\sim 23^\circ\text{C}$), as previously described⁷ using a T-format Quanta Master QM-9 photon counting fluorometer (1-nm steps, 2-nm slits) operated with Felix software (Photon Technology International, Lawrenceville, New Jersey). The quantum yield of fluorocoxib A was calculated by comparison with the fluorescence of 5-ROX as previously reported.⁸ The extinction coefficients (ϵ) of fluorocoxib A and 5-ROX [Fig. 1(e)] were calculated from absorbance spectra of solutions (2 to $10 \mu\text{M}$) measured in 10-mm pathlength cuvettes recorded with a UV-VIS spectrophotometer (UV-2501PC, Shimadzu Corp.).⁸

As an *in vitro* model retinal tissue culture system for studying COX-2 induction and fluorocoxib A binding specificity, we used R28 rat retinal cells. R28 cells were grown in Dulbecco's Modified Eagle medium, high glucose, with 10% fetal bovine serum in 150-mm plates until they reached 30% confluence. The cells were treated with tumor necrosis factor-alpha (TNF α) at 5 ng/mL for 18 h to induce COX-2, and protein was isolated from lysates using the M-PerTM mammalian protein isolation kit (ThermoFisher). Lysate protein (20 μg) was

*Address all correspondence to: Md. Jashim Uddin, E-mail: jashim.uddin@vanderbilt.edu

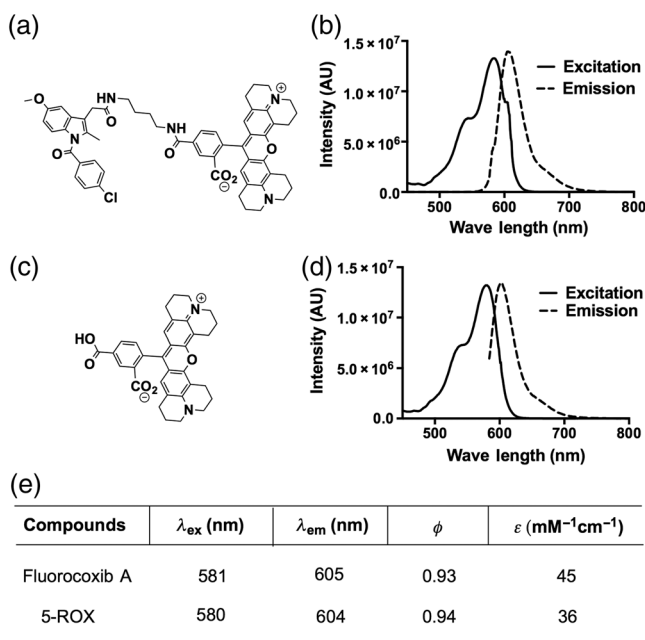


Fig. 1 Photophysical properties of fluorocoxib A and 5-ROX. Structures of (a) fluorocoxib A and (c) 5-ROX, steady state fluorescence excitation and emission spectra were determined for (b) fluorocoxib A and (d) 5-ROX in buffer, pH 7, using a Spex 1681 Fluorolog spectrofluorometer, equipped with a 450-W xenon arc lamp, and (e) data table.

loaded on a 7.5% SDS/PAGE resolving gel and transferred onto 0.2 μ m nitrocellulose, which was then probed with a rabbit antibody against murine COX-2 followed by a secondary horseradish peroxidase-conjugated anti-rabbit IgG antibody. The western blot revealed a band that correlated with a standard mCOX-2 protein band, suggesting that TNF α treatment induces elevation of COX-2 expression in these cells [Fig. 2(a)].

The *in vitro* COX-2 inhibitory activities of fluorocoxib A and 5-ROX were evaluated using a purified protein assay similar to that described previously.⁶ Briefly, reaction mixtures (200 μ L) containing hematin-reconstituted COX-2 (60 nM) in 100 mM Tris-HCl, pH 8.0, and 500 μ M phenol, were preincubated with varying concentrations of fluorocoxib A or 5-ROX (added as stock solutions in dimethylsulfoxide) at 25°C for 17 min and 37°C for 3 min followed by the addition of 5 μ M [1-¹⁴C]arachidonic acid (¹⁴C-AA, ~5 to 7 mCi/mmol, Perkin Elmer). After termination of the reaction with the addition of ether:methanol:citric acid (30:4:1), the phases were separated, and the organic phase was spotted on a thin-layer chromatography (TLC) plate and developed to separate radiolabeled products, which were quantified by a radioactivity scanner. Fluorocoxib A exhibited selective COX-2 inhibition with an IC₅₀ value of 0.12 μ M, whereas 5-ROX showed no inhibitory activity [Fig. 2(b)].

The binding specificity of fluorocoxib A to COX-2 in inflammatory R28 cells was also studied using radioactivity assays. Cells at 30% confluence were treated with TNF α (5 ng/mL) and incubated for 18 h. Next, the cells were washed and overlaid with a serum-free medium containing the desired concentrations of fluorocoxib A or 5-ROX dissolved in dimethyl sulfoxide and preincubated for 30 min at 37°C followed by addition of ¹⁴C-AA (5 μ M) for 30 min at 37°C. The reaction was terminated with ether:methanol:citric acid (30:4:1), the phases were separated,

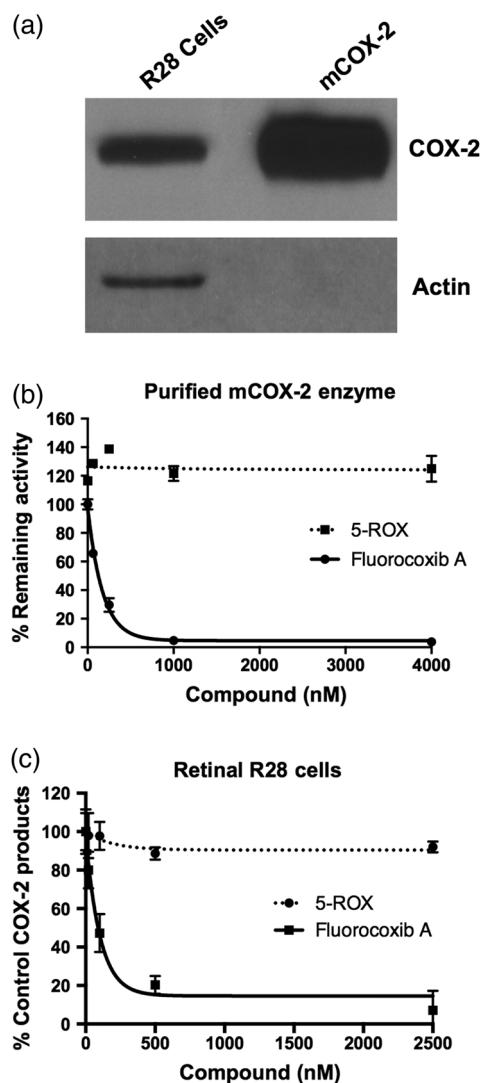


Fig. 2 Expression and inhibition of COX-2. (a) Expression of COX-2 in TNF α -treated retinal R28 cells. Effects of 5-ROX and fluorocoxib A on COX-2 activity in (b) a purified enzyme preparation and (c) intact R28 cells.

and the organic phase was spotted on TLC plates. The plates were developed in ethyl acetate/dichloromethane/acetic acid (75:25:1), and radiolabeled products were quantified with a radioactivity scanner. In this cell-based assay, fluorocoxib A inhibited COX-2 in TNF α -activated R28 cells (IC₅₀ = 0.08 μ M), but 5-ROX was inactive [Fig. 2(c)].

The COX-2-targeting potential of fluorocoxib A was next evaluated in the LCNV mouse model. In this model, an argon laser is used to induce several laser burns in the subretinal space *via* perforation of Bruch's membrane, which is associated with early inflammation mediated by COX-2 derived prostaglandins 1 to 3 days post laser injury, with subsequent choroidal neovascularization in later stages of the model (days 5 to 7).⁹ All animal procedures were performed in accordance with the Institutional Animal Care and Use Committee (IACUC) at Vanderbilt University Medical Center. LCNV lesions were generated bilaterally in three groups of six C57BL/6J female mice using an argon laser photocoagulator (blue-green light) mounted on a slit-lamp (Nidek SL-1600). The focal laser was applied concentrically (100- μ m spot size, 0.1-s duration, 0.1 W),

approximately two optic discs from the center, avoiding major blood vessels of each eye. Up to five lesions were induced in each eye successfully as indicated by visualization of a cavitation bubble in the subretinal space upon laser irradiation, which is consistent with an 80% to 90% average success rate of laser injury in this model. Three mice were nonlaser treated to correct for autofluorescence using matched 5-ROX detection settings in treated animals.

At 24-h postlaser injury, each group of six animals received intraperitoneal injections of either fluorocoxib A (1 mg/kg), 5-ROX dye (1 mg/kg), or fluorocoxib A (1 mg/kg) in animals pretreated with celecoxib (10 mg/kg, i.p.) 1 h prior to injection to neutralize COX-2 binding. At 3-h postinjection, both eyes of each mouse were imaged using the Micron III retinal fluorescence imaging system (Phoenix Research Systems, Inc.) using a 5-ROX excitation and emission filter set (Semrock Technologies, Inc.) with identical exposure and gain settings for each group of animals. Nonlaser-treated, uninjected animals were used to ensure that 5-ROX emission in the retina was below the threshold of detection.

In each experimental group, at least 40 lesions were selected for postacquisition image analysis. For analysis of signal-to-background ratios of imaging agents and controls, average fluorescence pixel intensity (in the 5-ROX acquisition channel) was measured in each LCNV lesion using Image Pro Plus 7 software, although freely available image analysis packages can be used for the same pixel analysis. Region of interest (ROI) demarcation of each lesion was limited to the 100- μ m spot size of the laser injury, and LCNV burns were identified using the corresponding brightfield image. Average pixel intensity in equivalently defined 100 μ m ROIs in adjacent healthy retinal tissue not affected by the laser burn two optic disc diameters radially from the optic disc was used to determine signal-to-background ratios. The ROI values in photons/s of a typical LCNV lesion and a normal retinal tissue were measured as 2.373×10^{10} and 1.230×10^9 , respectively.

In laser-treated mice, COX-2 expression was specifically detected by fluorocoxib A, consistent with previous studies in tumor models, as exhibited by an approximately 16-fold signal-to-background ratio enhancement over dye only or COX-2 competitive inhibition controls (Fig. 3). 5-ROX emission from fluorocoxib A was focally localized to the inflammatory lesions induced by laser administration, and binding of molar-equivalent dye 5-ROX was negligible as indicated by signal-to-noise ratios comparable to background mouse retinas (uninjected, nonlaser-treated mice imaged in 5-ROX channel). Pretreatment with celecoxib, an inhibitor of COX-2, prevented fluorocoxib A-mediated detection of COX-2 *via* competitive inhibition of the matched target.

Detectable COX-2 expression from fluorocoxib A emission was observed within the optic disc [Fig. 3(b)]. Although the optic disc was nonlaser-treated, it is likely that proximal laser burns also induced inflammation within the optic nerve, which is susceptible to inflammatory stress, as observed in optic neuritis, glaucoma, and multiple sclerosis. Specifically, COX-2 is known to be induced in optic neuritis as observed in human specimens,¹⁰ and even in unaffected human specimens, low but detectable levels of COX-2 were observed in the optic nerve. Also, in other works,¹¹ COX-2 was localized to a few cells in the optic nerve head of glaucomatous patient tissue specimens, with low but detectable expression in normal optic nerve tissue. We plan to investigate optic nerve expression of COX-2 in future

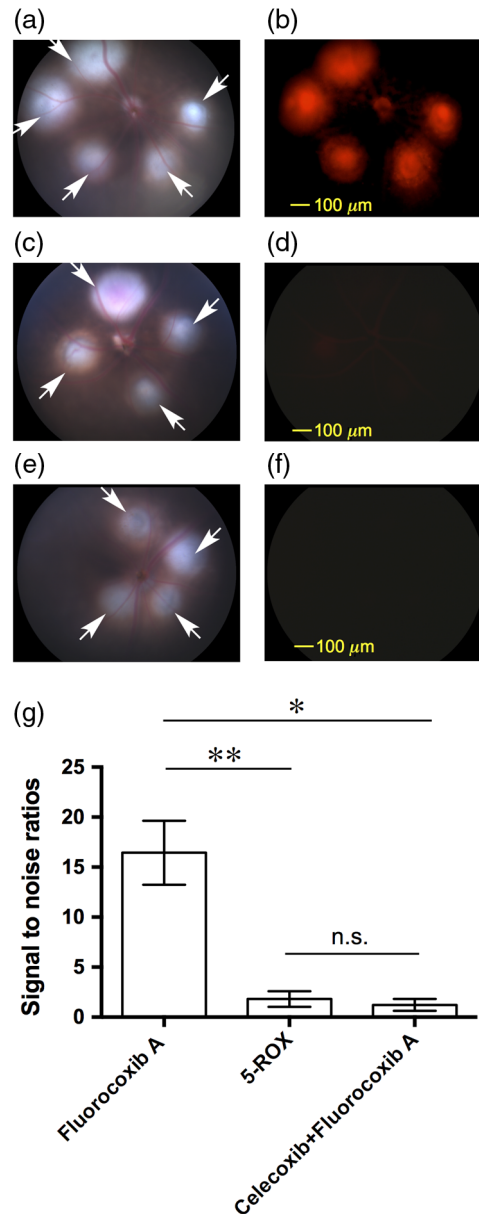


Fig. 3 *In vivo* imaging of COX-2 using fluorocoxib A in a mouse model of LCNV. (a)–(f) Corresponding brightfield and 5-ROX emission channel images of retinas in mice injected with (a) and (b) fluorocoxib A, (c) and (d) 5-ROX dye, and (e) and (f) celecoxib + fluorocoxib A. (g) Signal-to-noise calculations based on average pixel intensities in LCNV and adjacent healthy tissue in 5-ROX emission channel ($n = 6$ per group). * $p < 0.001$; ** $p < 0.01$

longitudinal studies within LCNV and glaucoma mouse models to further validate COX-2 expression in the optic nerve as a potential imaging biomarker for early detection and staging of retinal diseases, which involve optic neuropathies.

In this work, we have demonstrated selective accumulation of fluorocoxib A in LCNV lesions as compared to surrounding normal noninflamed retinal tissues. The COX-2-dependence of fluorocoxib A uptake within retinal vascular lesions induced by laser treatment was validated by imaging with the nontargeted 5-ROX dye and by preblocking the COX-2 active site with celecoxib, both of which resulted in little uptake of fluorescent COX-2 targeted compound. These findings strongly support the hypothesis that COX-2 is an ideal molecular imaging target

for early diagnosis and monitoring of inflammatory retinal vascular diseases, in which fluorocoxib A or its near-infrared derivatives can play a vital role, in preclinical and clinical settings. Also, COX-2 may be a valuable molecular imaging biomarker for early detection of retinal diseases, staging of disease severity, and monitoring therapeutic response in patients with retinal disease including AMD and diabetic retinopathy.¹²

Acknowledgments

We are grateful to the National Institutes of Health [Grant Nos. CA128323-4,-5 (MJU), CA182850-01A1 (MJU), CA136465 (LJM), CA89450 (LJM), and EY023397 (AJ)] for financial support for this study. We thank the Molecular Physiology and Biophysics (MPB) Fluorescence Spectroscopy Core Lab for the use of the PTI photon counting fluorometer and Dr. Charles Cobb for advice on its use. We are grateful to Dr. Shu Xu of the Department of Biochemistry for assistance with text formatting and to Dr. Carol A. Rouzer of the Vanderbilt Institute for Chemical Biology for critical reading of this manuscript.

References

1. F. L. Ferris, S. L. Fine, and L. Hyman, "Age-related macular degeneration and blindness due to neovascular maculopathy," *Arch. Ophthalmol.* **102**(11), 1640–1642 (1984).
2. K. B. Freund, L. A. Yannuzzi, and J. A. Sorenson, "Age-related macular degeneration and choroidal neovascularization," *Am. J. Ophthalmol.* **115**(6), 786–791 (1993).
3. L. A. Donoso et al., "The role of inflammation in the pathogenesis of age-related macular degeneration," *Surv. Ophthalmol.* **51**(2), 137–152 (2006).
4. Y. Wang, V. M. Wang, and C. C. Chan, "The role of anti-inflammatory agents in age-related macular degeneration (AMD) treatment," *Eye (Lond)* **25**(2), 127–139 (2011).
5. S. C. Maloney et al., "Expression of cyclooxygenase-2 in choroidal neovascular membranes from age-related macular degeneration patients," *Retina* **29**(2), 176–180 (2009).
6. M. J. Uddin et al., "Selective visualization of cyclooxygenase-2 in inflammation and cancer by targeted fluorescent imaging agents," *Cancer Res.* **70**(9), 3618–3627 (2010).
7. J. O. McIntyre et al., "Development of a novel fluorogenic proteolytic beacon for in vivo detection and imaging of tumour-associated matrix metalloproteinase-7 activity," *Biochem. J.* **377**(Pt. 3), 617–628 (2004).
8. M. J. Uddin and L. I. Marnett, "Synthesis of 5- and 6-carboxy-X-rhodamines," *Org. Lett.* **10**(21), 4799–4801 (2008).
9. S. J. Kim et al., "Ketorolac inhibits choroidal neovascularization by suppression of retinal VEGF," *Exp. Eye Res.* **91**(4), 537–543 (2010).
10. V. L. Tsoi et al., "Immunohistochemical evidence of inducible nitric oxide synthase and nitrotyrosine in a case of clinically isolated optic neuritis," *J. Neuroophthalmol.* **26**(2), 87–94 (2006).
11. A. H. Neufeld et al., "Cyclooxygenase-1 and cyclooxygenase-2 in the human optic nerve head," *Exp. Eye Res.* **65**(6), 739–745 (1997).
12. S. E. Yanni, G. W. McCollum, and J. S. Penn, "Genetic deletion of COX-2 diminishes VEGF production in mouse retinal Muller cells," *Exp. Eye Res.* **91**(1), 34–41 (2010).